Journal of Statistical Physics, Vol. 15, No. 4, 1976

Successive Bifurcations Leading to Stochastic Behavior

John McLaughlin[1]

Received February 13, 1976

A model of interacting normal modes in a nonlinear, dissipative system is constructed in order to analyze speculations by Ruelle and Takens. The first bifurcation leads to a periodic state. The second bifurcation leads to phaselocking, if the first mode is sufficiently energetic. A third bifurcation leads to stochastic behavior. Possible relevance of these phenomena for physical systems is discussed.

KEY WORDS: Bifurcation; correlation function; dissipative; nonlinear; nonperiodic; normal mode; quasiperiodic; stochastic; turbulence.

1. INTRODUCTION

Ruelle and Takens[1] have speculated that certain fluid mechanical systems, such as Couette flow, may enter stochastic states through a small number of bifurcations. At each bifurcation, a new frequency appears in the flow. However, nonlinear interactions between three or four normal modes are supposed to create nonperiodic time dependence. Ruelle and Takens suggest that the dynamical variables of the system will be "mixing," meaning that their time correlation functions will go to zero as the time displacement goes to infinity. Actually, the more common usage of the term "mixing" refers to a somewhat more general property of measure-preserving systems.[2] However, in this paper, "mixing" will be used as shorthand for variables whose autocorrelation functions go to zero as the time displacement approaches infinity.

Unfortunately, Ruelle and Takens offer no examples of the above behavior. Furthermore, although their arguments use topological ideas to suggest "generic" behavior, it is questionable whether mechanical systems happen to lie within such "generic classes." However, the basic idea that very simple mathematical systems can be mixing is correct. For example, consider the so-called "c-systems."[2] The c-systems are measure-preserving systems

[1] Physics Department, Clarkson College of Technology, Potsdam, New York.

in which all orbits are highly unstable. It can be rigorously proved[2] that the orbital instability implies that the systems are mixing.

The c-systems are more than mathematical abstractions. Orszag[3] has found an example of a c-system which consists of five nonlinearly coupled degrees of freedom. Using extremely accurate numerical techniques, Orszag found that all orbits of the system were unstable, and that the autocorrelation function of each of the five modes goes to zero.

Unfortunately, very little is known about nonlinear dissipative systems. Lorenz[4] found a dissipative system, consisting of three nonlinearly coupled degrees of freedom, which exhibits highly aperiodic time dependence. The orbits of the system are attracted onto a complicated surface on which all orbits are highly unstable. Unpublished calculations by the author, using high-order predictor–corrector schemes, show that the Lorenz system is mixing.

The Lorenz system does not conform to the Ruelle–Takens picture. Ruelle and Takens deal with systems that exhibit "forward" bifurcations, which are nonhysteretic. The Lorenz system exhibits a "backward," or subcritical, bifurcation, which exhibitis hysteresis.

In a previous paper,[5] McLaughlin and Martin made a numerical study of a model of thermal convection in a fluid with low Prandtl number in Rayleigh–Benard geometry with free-slip boundaries. The Prandtl number σ is defined in terms of the kinematic viscosity ν and the thermal diffusivity κ by the expression

$$\sigma \equiv \nu/\kappa \tag{1}$$

The model system was obtained by making a severe spectral truncation of the Boussinesq equations. Despite the truncation, the system still exhibited behavior roughly similar to that found experimentally by Willis and Deardorff[6] and Ahlers.[7] The different regimes of the model are defined in terms of the Rayleigh number R,

$$R \equiv g\epsilon H^3 \Delta T/\kappa\nu \tag{2}$$

In Eq. (2), g is the acceleration of gravity, ϵ is the coefficient of thermal expansion, H is the thickness of the fluid layer, and ΔT is the difference between the temperatures of the lower and upper surfaces of the fluid layer.

The model yields convective motion in the form of straight rolls for Rayleigh numbers exceeding a critical value R_c,

$$R_c = 657 \tag{3}$$

The next transition occurs at $R = 1.24R_c$, where the straight rolls become unstable to wavy rolls. The motion is strictly periodic for an interval of

Rayleigh numbers above the second threshold. At $R = 1.6R_c$, an instability to highly aperiodic fluctuations was found. In the interval between $R = 1.24R_c$ and $1.6R_c$, there is still another bifurcation in which another wavelength starts to draw energy. This wavelength is not driven by the other modes (see Section 2), so that its Fourier components are strictly zero below the bifurcation. The fact that the second bifurcation leads to strictly periodic motion suggests that a phaselocking mechanism is at work.

It is not clear whether three or four bifurcations occur before the onset of aperiodicity seen at $R = 1.6R_c$. However, it was found that if the fourth spatial harmonics were dropped from the model, the system exhibited strictly periodic behavior at all Rayleigh numbers. This suggested that the ideas of Ruelle and Takens might apply to this model of convection.

There were several problems with the work on the convection model. First, the model was very crude. It is clearly desirable to study a more realistic model of low-Prandtl-number convection. The author is currently undertaking this work, and the results will be reported elsewhere.

The single time step scheme used to integrate the equations was another weakness of the computations. This procedure has low accuracy, and it might be argued that the nonperiodicity found was produced by roundoff. This problem is amplified by the fact that each wave was represented by eight Fourier components. It is hoped that this resolution makes the model qualitatively realistic. However, it also raises the possibility that the noisy behavior was simply due to the large number of degrees of freedom (39) in the model.

In order to circumvent the above difficulties, a model will be exhibited in which each wave is represented by a single complex function of time. The waves will be coupled by a set of nonlinear ordinary differential equations, which are suggested by the convection equations in Ref. 5. The equations are then integrated, using highly accurate predictor–corrector schemes, and are found to exhibit behavior which conforms well with the Ruelle–Takens picture. In particular, the model exhibits phaselocking after two bifurcations and stochastic behavior after three bifurcations provided that a sufficient number of nonlinear couplings are present in the model.

2. REVIEW OF CONVECTION MODEL

Let us take the x and y axes to lie in a plane parallel to the surfaces of the convection layer. The z axis will be chosen so that the z coordinate of the lower surface is zero. It is possible to find solutions of the Boussinesq equations with straight rolls oriented parallel to any horizontal direction. For convenience, this direction will be chosen to be parallel to the x axis.

It is possible to convert the Boussinesq equations into an infinite set of

coupled, nonlinear ordinary differential equations by the following substitutions:

$$\mathbf{V}(\mathbf{r}, t) = i \sum_{\substack{l,m,n \\ l+n=\text{even}}} \mathbf{V}(l, m, n, t) F_{lmn}(x, y, z) \tag{4}$$

$$\theta(\mathbf{r}, t) = i \sum_{\substack{l,m,n \\ l+n=\text{even}}} (l, m, n, t) F_{lmn}(x, y, z) \tag{5}$$

$$F_{lmn}(x, y, z) = \exp[i(k_x l x + k_y m y + k_z n z)] \tag{6}$$

$$K_x \equiv 2\pi/\lambda_x, \qquad K_y \equiv 2\pi/\lambda_y, \qquad K_z \equiv \pi/H \tag{7}$$

The solutions in Eqs. (4) and (5) impose periodic boundary conditions over distances λ_x and λ_y in the x and y directions. It is a property of the Boussinesq equations that solutions with $l + n =$ even for all Fourier components can be found. Busse[8] has shown that these are the physically interesting solutions in the transition to time dependence for low-Prandtl-number fluids.

The values of the Fourier components cannot be chosen arbitrarily without violating either the reality of the velocity and temperature fields or the boundary conditions at the two surfaces of the fluid layer. The fields will be real if the following condition is imposed:

$$\mathbf{V}(-l, -m, -n, t) = -\mathbf{V}^*(l, m, n, t) \tag{8}$$

$$\theta(-l, -m, -n, t) = -\theta^*(l, m, n, t) \tag{9}$$

The asterisks in Eqs. (8) and (9) denote complex conjugation.

If free-slip boundary conditions are imposed, the following symmetries must be imposed on the Fourier components:

$$U(l, m, -n, t) = U(l, m, n, t) \tag{10}$$

$$V(l, m, -n, t) = V(l, m, n, t) \tag{11}$$

$$W(l, m, -n, t) = -W(l, m, n, t) \tag{12}$$

$$\theta(l, m, -n, t) = -\theta(l, m, n, t) \tag{13}$$

Let us consider the solution corresponding to straight convection rolls parallel to the x axis. In this case, m is zero, there is no y component of velocity and Eqs. (8)–(13) imply the following symmetries:

$$U(-l, 0, n, t) = -U^*(l, 0, n, t) \tag{14}$$

$$W(-l, 0, n, t) = W^*(l, 0, n, t) \tag{15}$$

$$\theta(-l, 0, n, t) = \theta^*(l, 0, n, t) \tag{16}$$

Inspection of the Boussinesq equations (see Ref. 5) reveals that the origin of coordinates can be chosen so that the Fourier components of the roll are real. In this case, Eqs. (14)–(16) can be replaced by the following relations:

$$U(-l, 0, n, t) = -U(l, 0, n, t) \tag{17}$$

$$W(-l, 0, n, t) = W(l, 0, n, t) \tag{18}$$

$$\theta(-l, 0, n, t) = \theta(l, 0, n, t) \tag{19}$$

Busse[8] identified the mode of instability that leads to the wavy rolls. The source of energy for the waves is the kinetic energy of the straight rolls. This energy is released through a shear instability of the rolls. This mechanism manifests itself in the fact that the wave fields have the symmetries of the x derivatives of the corresponding roll fields. Let us denote the wave fields by the subscript W:

$$U_W(-l, m, n, t) = U_W(l, m, n, t) \tag{20}$$

$$V_W(-l, m, n, t) = -V_W(l, m, n, t) \tag{21}$$

$$W_W(-l, m, n, t) = -W_W(l, m, n, t) \tag{22}$$

$$\theta_W(-l, m, n, t) = -\theta_W(l, m, n, t) \tag{23}$$

Traveling waves can be specified by the following conditions:

$$U_W(l, -m, n, t) = -U_W{}^*(l, m, n, t) \tag{24}$$

$$V_W(l, -m, n, t) = V_W{}^*(l, m, n, t) \tag{25}$$

$$W_W(l, -m, n, t) = -W_W{}^*(l, m, n, t) \tag{26}$$

$$\theta_W(l, -m, n, t) = -\theta_W{}^*(l, m, n, t) \tag{27}$$

Let us define all Fourier components having the symmetry of the roll field to be the background field, and denote them by the subscript B:

$$U_B(-l, m, n, t) = -U_B(l, m, n, t) \tag{28}$$

$$V_B(-l, m, n, t) = V_B(l, m, n, t) \tag{29}$$

$$W_B(-l, m, n, t) = W_B(l, m, n, t) \tag{30}$$

$$\theta_B(-l, m, n, t) = \theta_B(l, m, n, t) \tag{31}$$

$$U_B(l, -m, n, t) = U_B{}^*(l, m, n, t) \tag{32}$$

$$V_B(l, -m, n, t) = -V_B{}^*(l, m, n, t) \tag{33}$$

$$W_B(l, -m, n, t) = W_B{}^*(l, m, n, t) \tag{34}$$

$$\theta_B(l, -m, n, t) = \theta_B{}^*(l, m, n, t) \tag{35}$$

Letting ϕ_B and ϕ_W represent background and wave Fourier components, the nonlinear and linear terms of the Boussinesq equations are of the following form:

$$d\phi_B/dt = \phi_B\phi_B + \phi_W\phi_W + \phi_B \tag{36}$$

$$d\phi_W/dt = \phi_B\phi_W + \phi_W \tag{37}$$

Thus, for example, it is possible to find exact solutions of the Boussinesq equations in the form of Eqs. (4) and (5) with wave Fourier components having odd values of m and background Fourier components having only even values of m.

3. THE MODEL

The convection equations will serve as a guide in constructing a model exhibiting successive bifurcations. Let us assume that the fields can be split into "wave" and "background" fields. Each wave will be represented by a single complex function of time, and a single space dimension will be retained. We have

$$V_B(x, t) = \sum_m V_B(m, t)e^{ikmx} \tag{38}$$

$$V_W(x, t) = \sum_m V_W(m, t)e^{ikmx} \tag{39}$$

The following conditions guarantee that the physical space fields will be real, and that the waves will be traveling instead of standing (standing waves could be imposed by requiring the Fourier components to be real):

$$V_B(-m, t) = V_B{}^*(m, t) \tag{40}$$

$$V_W(-m, t) = W_W{}^*(m, t) \tag{41}$$

By analogy with Eqs. (36) and (37), let us study the following evolution equations:

$$dV_W(m)/dt = \sum_q V_W(q)V_B(m - q) - i\omega_m V_W(m) \tag{42}$$

$$dV_B(m)/dt = \sum_q V_W(q)V_W(m - q) + V_B(q)V_B(m - q) - \nu_m V_B(m) \tag{43}$$

The parameters ω_m will be taken to be complex numbers, and the parameters ν_m will be chosen to be real and positive. Thus, the $V_W(m)$ are oscillatory modes, which can be either growing or decaying, depending on the sign of $\omega_m{}^i$, in the linearized equations. The $V_B(m)$ are passive, nonoscillatory modes.

If the amplitudes of all the modes are infinitesimal, the stability of each wave is determined by the imaginary part of ω_m, ${\omega_m}^i$. For example, suppose that only ${\omega_1}^i$ is greater than zero. In that case, $V_W(1)$ will acquire a finite size, and will oscillate at roughly ${\omega_1}^r$. (The frequency is modified by the nonlinear terms.) Furthermore, $V_W(m)$ for m odd and $V_B(n)$ for n even will be nonlinearly driven by the first mode. This is easily verified either numerically or by a perturbation expansion in ${\omega_1}^i$.

Were it not for the primary mode, $V_W(2)$ would acquire a finite size when ${\omega_2}^i$ became positive. However, for the choice of ν_m to be used in this paper [see Eqs. (63) and (64)], the distortions produced on the background field by the primary mode have the effect of suppressing $V_W(2)$. This behavior can be studied analytically for small primary amplitudes. To first order in ${\omega_1}^i$, the primary mode is determined by the following expressions:

$$V_W(1) = |V_W(1)| \exp(-i\Omega_1 t) \tag{44}$$

$$|V_W(1)|^2 = \frac{{\omega_1}^i}{(1/\nu_0) - \{\nu_2/[{\nu_2}^2 + 4({\omega_1}^r)^2]\}} \tag{45}$$

$$\Omega_1 = {\omega_1}^r + |V_W(1)|^2\left[\frac{1}{\nu_0} + \frac{({\omega_1}^r)^2}{{\nu_2}^2 + ({\omega_1}^r)^2}\right] \tag{46}$$

To first order in ${\omega_1}^i$, only two background modes, $V_B(0)$ and $V_B(2)$, are nonzero:

$$V_B(0) = |V_W(1)|^2/\nu_0 \tag{47}$$

$$V_B(2) = [V_W(1)]^2/(\nu_2 - 2i{\omega_1}^r) \tag{48}$$

To second order in ${\omega_1}^i$, the linearized equations for $V_W(2)$ are as follows:

$$dV_W(2)/dt = [-V_B(0) - i\omega_2]V_W(2) + V_B(1)V_W(1) + V_B(3)V_W{}^*(1) \tag{49}$$

$$dV_B(1)/dt = 2V_W(2)V_W{}^*(1) + 2V_W(3)V_W{}^*(2) + 2V_B(2)V_B{}^*(1) + 2V_B(0)V_B(1) + 2V_B(3)V_B{}^*(2) - \nu_2 V_B(1) \tag{50}$$

$$dV_B(3)/dt = 2V_W(1)V_W(2) + 2V_B(1)V_B(2) + 2V_B(0)V_B(3) - \nu_3 V_B(3) \tag{51}$$

To first order in ${\omega_1}^i$, the threshold for the second mode is given by the following expression:

$${\omega_2}^i = |V_W(1)|^2\left[\frac{1}{\nu_0} - \frac{2\nu_2}{({\omega_2}^r - {\omega_1}^r)^2 + {\nu_2}^2} - \frac{2\nu_3}{({\omega_2}^r + {\omega_1}^r)^2 + {\nu_3}^2}\right] \tag{52}$$

The time dependence of the second mode above its threshold depends on the strength of the primary mode. This can be seen by examining Eqs. (49)–(51). If the equations are expanded to second order in ${\omega_1}^i$, an equation of the following form is obtained:

$$dV_W(2)/dt = [-i\omega_2 + \beta|V_W(1)|^2 + \gamma|V_W(1)|^4]V_W(2) + \delta[V_W(1)]^4 V_W{}^*(2) \tag{53}$$

The presence of the last term in Eq. (53) is very important. If the amplitude of $V_W(1)$ is very small, all powers of $V_W(1)$ can be dropped and the solution of Eq. (53) is simply

$$V_W(2) = A \exp(-i\omega_2 t) \tag{54}$$

The exponential growth of this solution will be saturated by nonlinear terms in A.

If $V_W(1)$ is finite, the solution in Eq. (54) will be modified by the addition of sum and difference frequencies. To second order in ${\omega_1}^i$, the solution will be of the following form:

$$V_W(2) = A \exp(-i\omega_2 t) + B \exp[-i(4\Omega_1 - \omega_2)t] \tag{55}$$

Such solutions have discrete frequency spectra, and are known as quasi-periodic functions.[9] It is easily verified that quasiperiodic functions can never be mixing.[9]

Above a certain threshold in $|V_W(1)|$, the linearized equations for $V_W(2)$ have another solution. This is a phase-locked solution in which $V_W(2)$ oscillates at exactly twice the frequency of $V_W(1)$:

$$V_W(2) = A \exp[(-2i\Omega_1 + {\Omega_2}^i)t] \tag{56}$$

$$A = |A| \exp(i\phi) \tag{57}$$

Substituting Eqs. (56) and (57) into Eq. (53), we obtain the following pair of equations for ${\Omega_2}^i$ and ϕ:

$${\omega_2}^r - 2\Omega_1 = \beta^i |V_W(1)|^2 + |V_W(1)|^4[\gamma^i - \delta^r \sin(2\phi) + \delta^i \cos(2\phi)] \tag{58}$$

$${\Omega_2}^i = {\omega_2}^i + \beta^r |V_W(1)|^2 + |V_W(1)|^4[\gamma^r + \delta^r \cos(2\phi) + \delta^i \sin(2\phi)] \tag{59}$$

Equation (58) can be solved for $\cos(2\phi)$. To leading order in ${\omega_1}^i$,

$$\cos(2\phi) = \frac{{\omega_2}^r - 2{\omega_1}^r}{|\delta|\,|V_W(1)|^4}\{\delta^r - [|\delta|^2 - ({\omega_2}^r - 2{\omega_1}^r)^2]^{1/2}\} \tag{60}$$

A phase-locked solution can only exist for $|V_W(1)|$ large enough that the cosine lies between -1 and 1. We have

$$|V_W(1)|^4 \geqslant \frac{|({\omega_2}^r - 2{\omega_1}^r)\{\delta^r - [|\delta|^2 - ({\omega_2}^r - 2{\omega_1}^r)^2]^{1/2}\}|}{|\delta|} \tag{61}$$

Note that if ${\omega_2}^r$ is very close to $2{\omega_1}^r$, phaselocking occurs at very small values of $|V_W(1)|$. Numerical integration reveals that the phase-locked solution is the only stable solution of the model soon, if not immediately, after its appear-

ance for the parameter choices of Section 5. The motion of the system is found to be exactly periodic with one period.

It seems plausible that the above mechanism may have produced the exact periodicity found after the second bifurcation in Ref. 5. Ruelle and Takens[1] also argue for phaselocking by applying Peixoto's theorem.

4. NUMERICAL TECHNIQUES

At this stage, it is convenient to discuss the numerical techniques used to integrate the model equations. Since the solutions to be discussed in the next section appeared to be stochastic, it was desirable to determine whether this behavior was due to roundoff error, truncation error in the integration scheme, or was a property of the true solutions of the equations. To this end, a variety of high-order predictor–corrector schemes were used to integrate the equations. These schemes used the Adams–Bashforth predictor and Adams–Moulton corrector.[10] The most accurate solutions were computed with the ninth-order (PECE) scheme in double precision (12 decimal places).

It must be pointed out that even the most accurate scheme does not yield accurate solutions over the integration times used in the calculation of correlation functions. This was checked by changing the initial conditions by one part in 10^{12} on two otherwise identical runs. The resulting orbits were identical to six decimal places over at least the first eight cycles of the first mode. However, when the same procedure was used on the long correlation function runs, the final values of the variables differed. Thus, it might be argued that the stochastic behavior, to be reported in the next section, was generated by roundoff. This is unlikely for two reasons. First, even over the time segments where the integration is accurate to six decimal places, the solutions exhibit the same unpredictability. The second reason is that the correlation functions changed by a statistically insignificant amount when the "noise" level was reduced by a factor 10^6. This was checked by running the same calculation with fourth- and ninth-order schemes (both in double precision). Using the error estimates in Ref. 10, it was found that the error produced by the ninth-order scheme was lower by a factor 10^6 than that of the four-order scheme. If it is assumed that the computational errors are responsible for the stochastic behavior, the correlation time should increase significantly when the errors are reduced by a factor 10^6. This was not the case. The correlation functions changed by an amount less than the statistical uncertainty produced by the finite length of the integration domain ($\sim 5\%$ of the mean squares for the runs in question).

Finally, all of the calculations were performed with a time step $\Delta t = 0.01$. This step size is roughly 0.5% of the cycle length for the fastest active mode in any of the calculations.

5. NONPERIODIC SOLUTIONS

After the second bifurcation, in which the even modes acquire nonzero values, all the modes are nonzero. This makes it more difficult to determine the location of subsequent bifurcations. However, the task of locating the third bifurcation is made easier if one works in the regime of phase-locked solutions. As $\omega_3{}^i$ is increased, a value is eventually reached where signs of aperiodicity begin to appear. The nonperiodicity is small at first in the sense that it occurs over time scales which are long compared to the periods of the three active modes. As $\omega_3{}^i$ is increased further, the nonperiodicity becomes more pronounced until it appears impossible to predict the motion even one "cycle" ahead.

In all of the calculations to be discussed, the real parts of the modal frequencies had the following values:

$$\omega_n{}^r = 0.2 + 0.8n \tag{62}$$

The damping of the background field was chosen as follows:

$$\nu_0 = 1 \tag{63}$$

$$\nu_n = n^2, \qquad n \geqslant 1 \tag{64}$$

The value of $\omega_1{}^i$ was set equal to unity,

$$\omega_1{}^i = 1 \tag{65}$$

Finally, the $\omega_n{}^i$ for $n > 4$ were calculated from $\omega_4{}^i$ by the following rule:

$$\omega_n{}^i = \omega_4{}^i - 2(n - 4), \qquad n > 4 \tag{66}$$

This ensured that the high-lying modes did not produce additional bifurcations.

It was found that the second bifurcation did not occur until $\omega_2{}^i$ was nearly unity. When $\omega_2{}^i$ was set equal to 1.4, $V_W(2)$ and $V_W(1)$ had roughly the same magnitude in the periodic regime. The first signs of nonperiodicity appear at around $\omega_3{}^i = 1.6$. It seems that the transition is sharp in the sense that nonperiodicity develops through a forward bifurcation as $\omega_3{}^i$ is increased. However, the transition is gradual in the sense that the correlation time goes to infinity as the bifurcation point is approached from above.

In order to determine whether the time dependence was quasiperiodic (discrete frequency spectrum) or nonperiodic (continuous frequency spectrum), the correlation functions of the modes were computed. For example, when $\omega_3{}^i = 2$, $\omega_4{}^i = 0$, and the system is truncated to $m \leqslant 12$, the orbits of the variables are highly unpredictable. The autocorrelation functions of the real parts of $V_W(1)$ and $V_W(2)$ are shown in Figs. 1 and 2. The integrals were

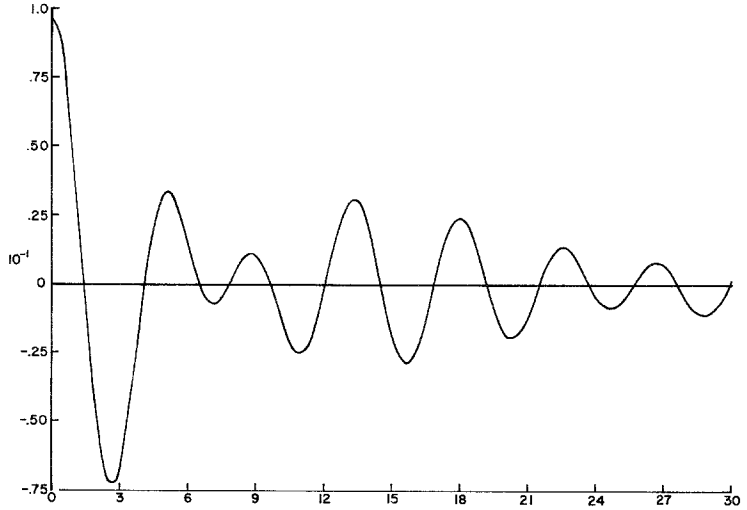

Fig. 1. Autocorrelation function of the real part of $V_W(1)$ [$V_W{}^r(1)$]. $m \leqslant 12$. $\omega_1{}^i = 1$, $\omega_2{}^i = 1.4$, $\omega_3{}^i = 2.0$, $\omega_4{}^i = 0$.

evaluated using a time range of 1500. Thus, roughly 250 cycles of $V_W(1)$ were included in the domain of integration. The fact that the autocorrelation function of $V_W(1)$ does not go to zero is due to the finite domain of integration, as will be shown later.

Note that the autocorrelation function of $V_W(2)$ decays much more slowly

Fig. 2. Maxima of the autocorrelation function of $V_W{}^r(2)$. $m \leqslant 12$. $\omega_1{}^i = 1$, $\omega_2{}^i = 1.4$, $\omega_3{}^i = 2.0$, $\omega_4{}^i = 0$.

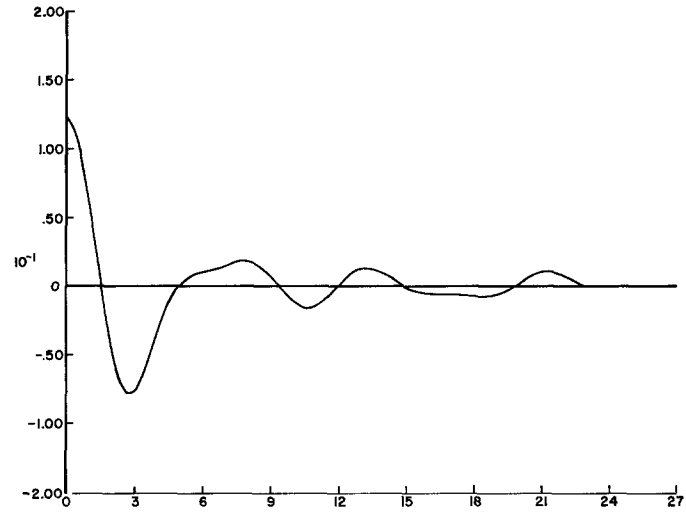

Fig. 3. Autocorrelation function of $V_W{}^r(1)$. $m \leqslant 4$. $\omega_1{}^i = 1$, $\omega_2{}^i = 1.4$, $\omega_3{}^i = 1.8$, $\omega_4{}^i = -0.2$.

than the others. This is probably a peculiarity of the model. Inspection of the time dependence of $V_W(2)$ shows that, although the succeeding maxima show great variation and unpredictability, the cycle lengths are almost constant (~ 3.2). This will be discussed in more detail later.

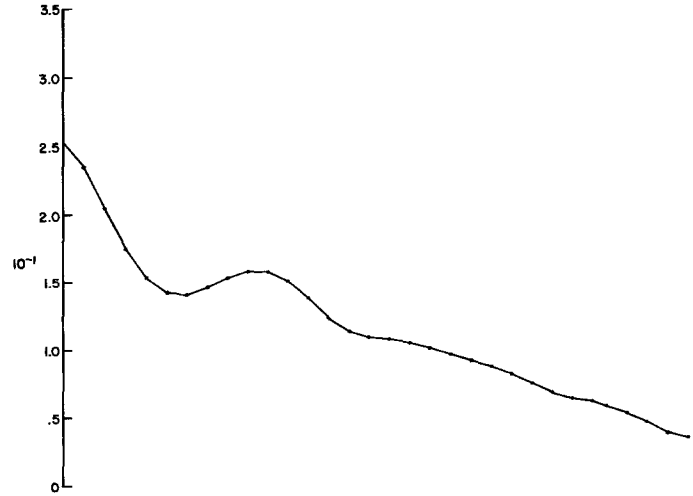

Fig. 4. Maxima of the autocorrelation function of $V_W{}^r(2)$. $m \leqslant 4$. $\omega_1{}^i = 1$, $\omega_2{}^i = 1.4$, $\omega_3{}^i = 1.8$, $\omega_4{}^i = -0.2$.

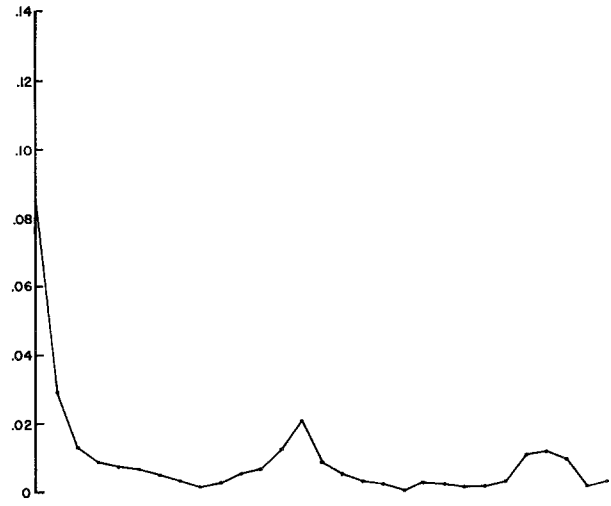

Fig. 5. Maxima of the autocorrelation function of $V_W{}^r(1)$. $m \leqslant 3$. $\omega_1{}^i = 1$, $\omega_2{}^i = 1.4$, $\omega_3{}^i = 1.8$.

In order to determine the effects of truncation and nonlinear interactions, the model was truncated to $m \leqslant 4$. When $\omega_1{}^i = 1$ and $\omega_2{}^i = 1.4$, non-periodicity was found to develop at somewhat smaller values of $\omega_3{}^i$. Figures 3 and 4 show the autocorrelation functions of $V_W{}^r(1)$ and $V_W{}^r(2)$ for $\omega_3{}^i =$

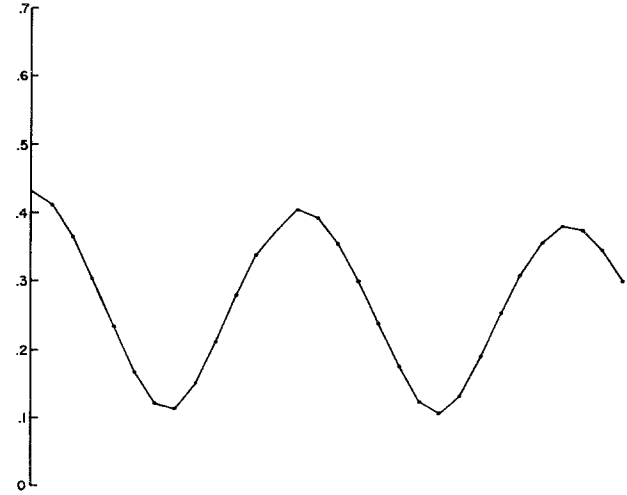

Fig. 6. Maxima of the autocorrelation function of $V_W{}^r(2)$. $m \leqslant 3$. $\omega_1{}^i = 1$, $\omega_2{}^i = 1.4$, $\omega_3{}^i = 1.8$.

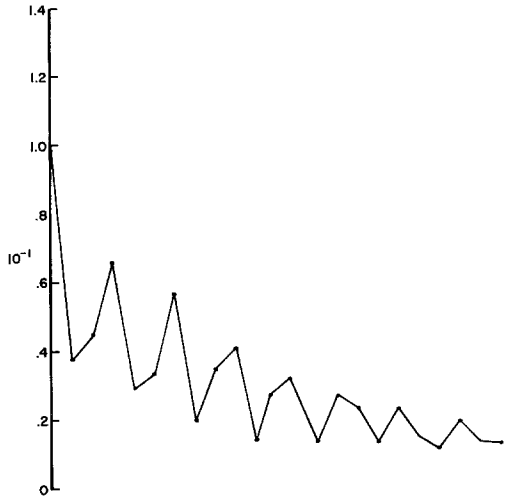

Fig. 7. Maxima of the autocorrelation function of $V_W{}^r(1)$. $m \leqslant 4$. $\omega_1{}^i = 1$, $\omega_2{}^i = 1.2$, $\omega_3{}^i = 1.8$, $\omega_4{}^i = -0.2$.

1.8 and $\omega_4{}^i = -0.2$. The calculations were repeated with $m \leqslant 3$. The results are shown in Figs. 5 and 6. Note that strong correlations recur over long times in this case.

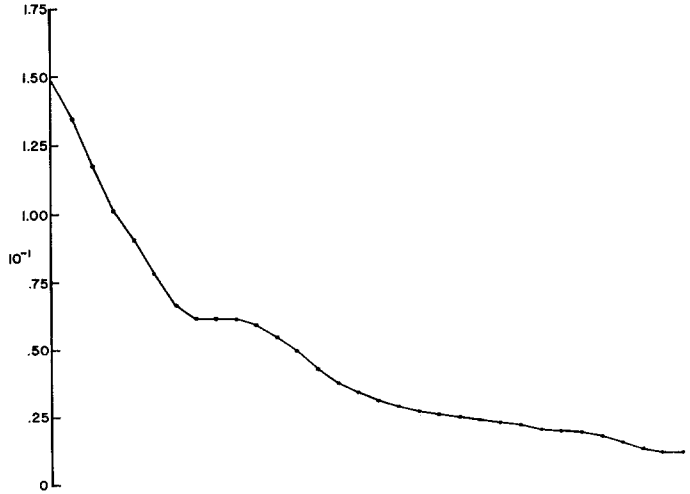

Fig. 8. Maxima of the autocorrelation function of $V_W{}^r(2)$. $m \leqslant 4$. $\omega_1{}^i = 1$, $\omega_2{}^i = 1.2$, $\omega_3{}^i = 1.8$, $\omega_4{}^i = -0.2$.

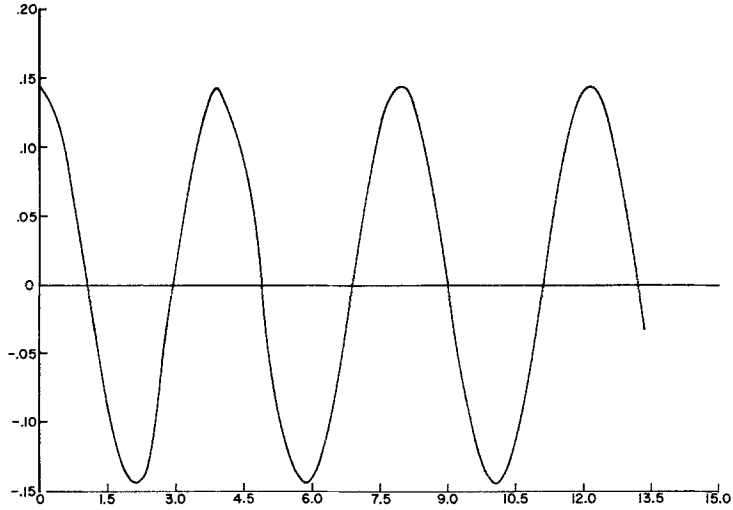

Fig. 9. Autocorrelation function of $V_W{}^r(1)$. $m \leqslant 3$. $\omega_1{}^i = 1$, $\omega_2{}^i = 1.2$, $\omega_3{}^i = 1.8$.

In order to check the generality of the above behavior, another set of runs was made with $\omega_1{}^i = 1$, $\omega_2{}^i = 1.2$, $\omega_3{}^i = 1.8$, and $\omega_i(4) = -0.2$. The results for $m \leqslant 4$ and 3 are shown in Figs. 7–9. It appears that the nonlinear interactions provided by the presence of the (passive) fourth mode are important in producing nonperiodicity. This sheds light on the results reported in Ref. 5. In those calculations, it was found that, upon removing the Fourier components comprising the fourth harmonic in a set of four nonlinearly interacting waves, the system reverted from nonperiodicity to periodicity. Nonperiodic solutions could not be found by varying the Rayleigh number in the three-wave system. The model calculations indicate that this was due to the lack of important nonlinear couplings rather than the inability of the system to produce a fourth bifurcation.

The fact that the autocorrelation function of $V_W(2)$ decays more slowly than those of $V_W(1)$, $V_W(3)$, and $V_W(4)$ in the calculations reported above seems related to the fact that there is a more direct link between $V_W(1)$ and $V_W(3)$ than there is between either of these two and $V_W(2)$. In order to test this, a fourth bifurcation was produced by increasing $\omega_4{}^i$, with $\omega_1{}^i = 1$, $\omega_2{}^i = 1.2$, and $\omega_3{}^i = 1.6$. The fourth mode bifurcates at roughly $\omega_4{}^i = 1.6$ and increases by a factor of four in magnitude when $\omega_4{}^i = 1.8$. In the latter case, all four modes have great variability in cycle length. The autocorrelation functions decay quickly toward zero. This is shown by Figs. 10 and 11. This computation was done in double precision with the ninth-order scheme. In order to check the mixing, the computation was repeated with an integration

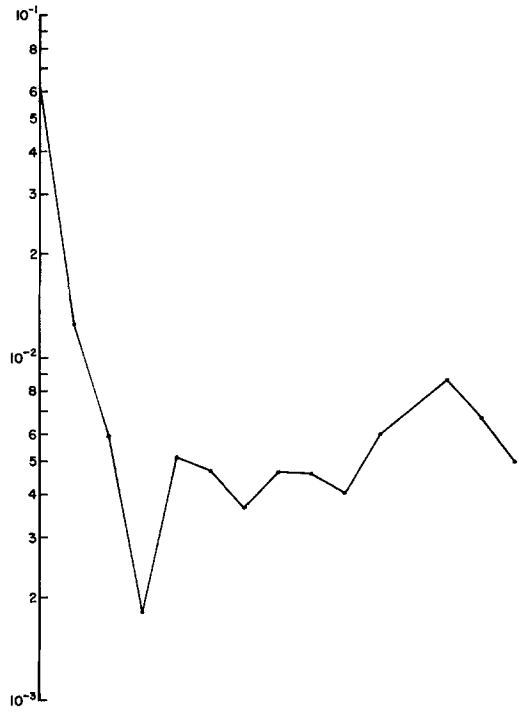

Fig. 10. Maxima of the autocorrelation function of $V_W{}^r(1)$. $m \leqslant 4$. $\omega_1{}^i = 1$, $\omega_2{}^i = 1.2$, $\omega_3{}^i = 1.6$, $\omega_4{}^i = 1.8$.

domain four times longer. [Thus, the domain was $\Delta t = 6000 \approx 1000$ cycles of $V_W(1)$.] It can be seen in Figs. 12 and 13 that the correlation functions mix down by an additional factor of two. This is determined by comparing the largest values of the correlation functions in their tail regions. The largest "tail region" values of the autocorrelation functions for $V_W{}^r(1)$ and $V_W{}^r(2)$ were 8.7×10^{-3} and 1.0×10^{-2} for the short run. These values were replaced by 3.1×10^{-3} and 5.5×10^{-3} on the long run.

Finally, as a check on the effect of computation error, the calculation in Figs. 12 and 13 was repeated with a fourth-order scheme. The results are displayed in Figs. 14 and 15. Note that the correlation functions mix down to almost exactly the same level (3.1×10^{-3} and 5.5×10^{-3} compared with 3.4×10^{-3} and 4.8×10^{-3}). On the other hand, the error produced by the fourth-order scheme is a factor 10^6 larger than that of the ninth-order scheme. Thus, it seems highly unlikely that the mixing behavior is due to computational error.

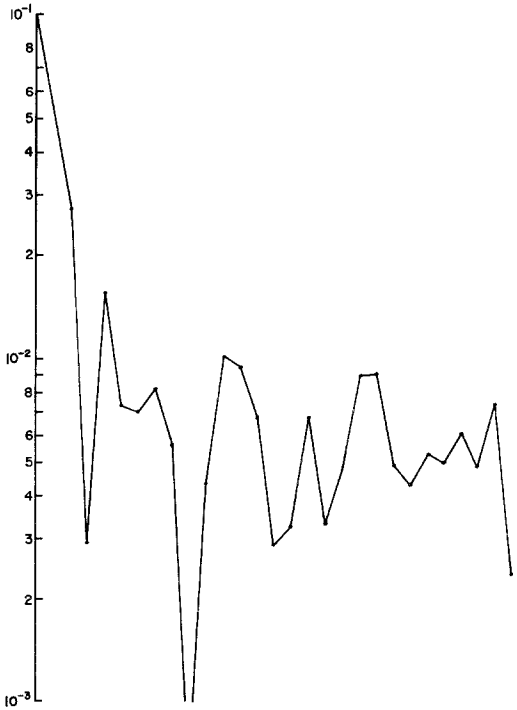

Fig. 11. Maxima of the autocorrelation function of $V_W{}^r(2)$. $m \leqslant 4$. $\omega_1{}^i = 1$, $\omega_2{}^i = 1.2$, $\omega_3{}^i = 1.6$, $\omega_4{}^i = 1.8$.

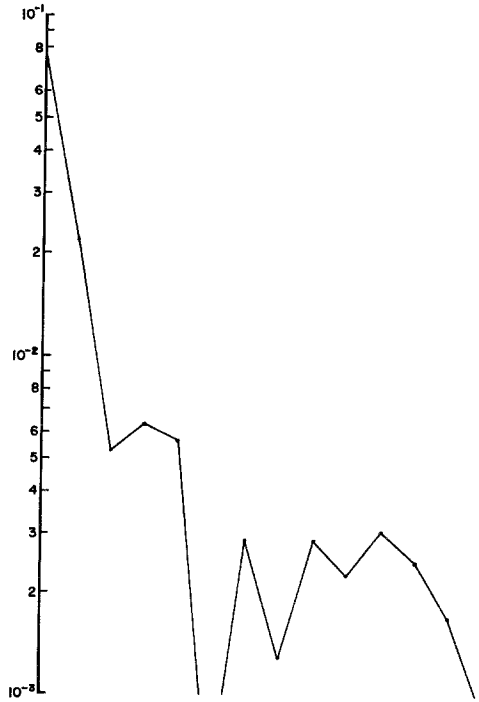

Fig. 12. Same as Fig. 10 but with integration time four times longer.

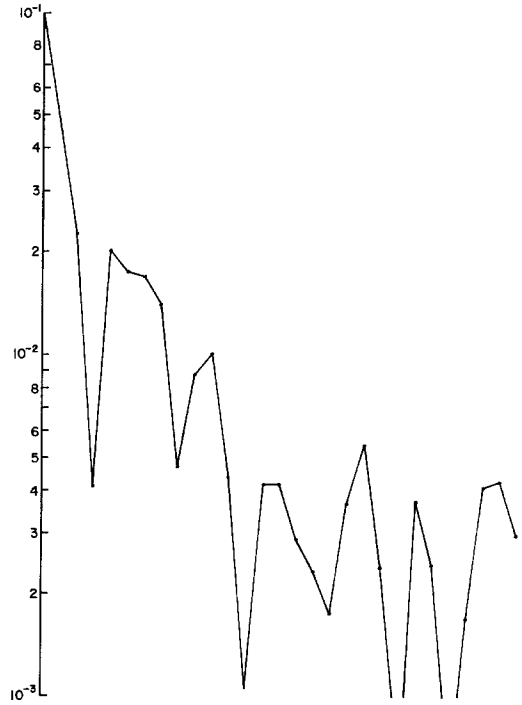

Fig. 13. Same as Fig. 11 but with integration time four times longer.

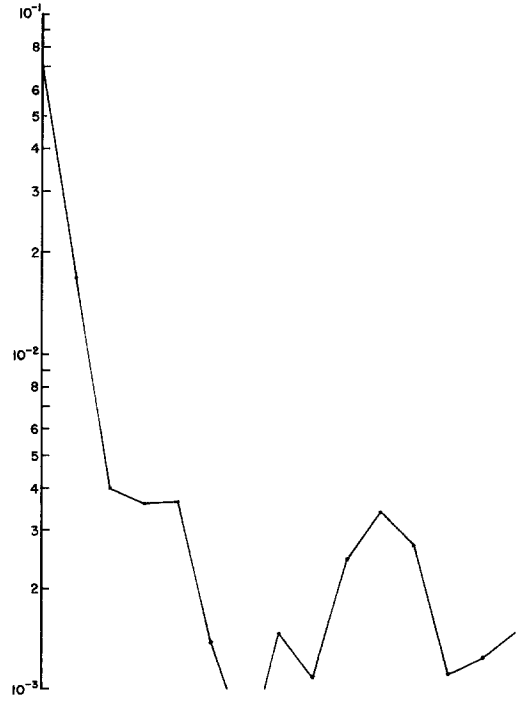

Fig. 14. Same as Fig. 12 but with fourth-order scheme (error larger by 10^6).

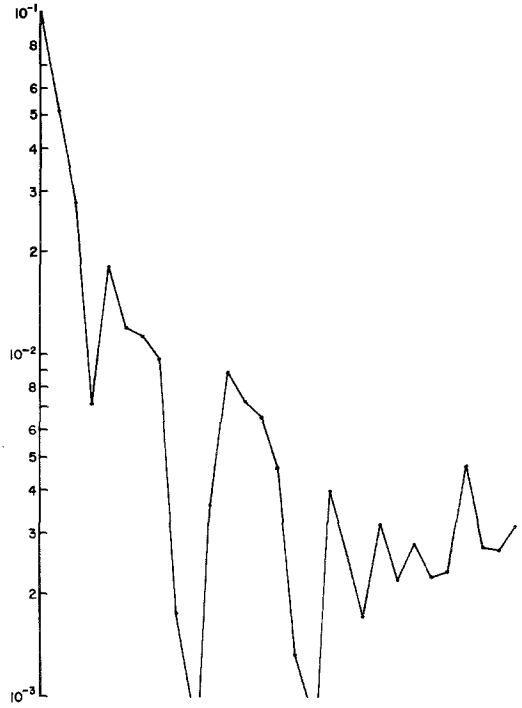

Fig. 15. Same as Fig. 13 but with fourth-order scheme (error larger by 10^6).

6. DISCUSSION

It has been shown that stochastic behavior can result through three forward bifurcations in a nonlinear, dissipative model system. Whether this will actually occur in physical systems is a much more difficult question. However, it is useful to discuss the kinds of systems to which these results might apply. The main requirement is that the system, when linearized about some time-independent "ground state," should have many normal modes with complex frequencies. As some external forcing parameter (e.g., Rayleigh number) is increased, the imaginary parts of the various frequencies become positive. Of course as soon as one mode develops a finite strength, the subsequent bifurcation points will be moved. In the model system of this paper, there is a one-to-one correspondence between the bifurcations of the nonlinear states and those predicted by the linearized problems. However, this is probably not crucial to the phenomena discussed.

Without doubt, the nonlinear couplings between modes are the most important factor in the onset of stochastic behavior. These couplings must

allow the time dependence of one mode to modify the time dependence of the other modes, and not just their amplitudes. In the case of traveling waves bifurcating on a one-dimensional, translationally invariant background field, this requirement boils down to demanding that the wave numbers be rationally related. This, in turn, will be satisfied if the system obeys periodic boundary conditions.

The behavior of the model discussed in this paper raises some interesting questions. Can the same sequence of phenomena occur in a system of equations derived from the model equations by perturbation expansion in the modal strengths? This would generalize the results somewhat. It could also reduce the dimensionality of the phase space to three, which would be interesting in view of Lorenz's work.[4]

What is the probability distribution of the fluctuations? Ruelle[11] has attacked the question of the existence of the probability distribution, but nothing is known of its nature.

Finally, and most interesting from the physicist's point of view, do these phenomena occur in physical systems? It is hoped that accurate numerical studies of Couette flow and low-Prandtl-number convection presently underway will answer this question for two plausible candidates.

ACKNOWLEDGMENTS

The author would like to thank S. Orszag for several helpful discussions and A. Garcia for assistance with the machine calculations.

REFERENCES

1. D. Ruelle and F. Takens, *Commun. Math. Phys.* **20**:167 (1971).
2. V. I. Arnold and A. Avez, *Ergodic Problems of Classical Mechanics*, W. A. Benjamin (1968).
3. S. A. Orszag, *Lectures on the Statistical Theory of Turbulence* (1973).
4. E. N. Lorenz, *J. Atmos. Sci.* **20**:130 (1963).
5. J. B. McLaughlin and P. C. Martin, *Phys. Rev. A* **12**:186 (1975).
6. G. E. Willis and J. W. Deardorff, *J. Fluid Mech.* **44**:661 (1970).
7. G. Ahlers, *Phys. Rev. Lett.* **33**:1185 (1974).
8. F. H. Busse, *J. Fluid Mech.* **52**:1, 97 (1972).
9. N. Wiener, *Acta Mathematica* **55**:117 (1930).
10. L. Lapidus and J. H. Seinfeld, *Numerical Solution of Ordinary Differential Equations*, Academic Press (1971).
11. D. Ruelle, "A Measure Associated with Axiom-A Attractors," preprint.